

# Thermoplastic Elastomer Hydrogels via Self-Assembly of an Elastin-Mimetic Triblock Polypeptide\*\*

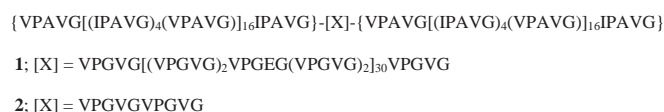
By Elizabeth R. Wright, R. Andrew McMillan, Alan Cooper, Robert P. Apkarian, and Vincent P. Conticello\*

Protein-based analogues of conventional thermoplastic elastomers can be designed with enhanced properties as a consequence of the precise control of primary structure. Protein **1** undergoes a reversible sol–gel transition, which results in the formation of a well-defined elastomeric network above a lower critical solution temperature. The morphology of the network is consistent with selective microscopic phase separation of the endblock domains. This genetic engineering approach provides a method for specification of the critical architectural parameters, such as block length and sequence, which define macromolecular properties that are important for downstream applications.

## 1. Introduction

Synthetic polymers consisting of well-defined blocks of compositionally dissimilar monomers undergo microscopic phase separation in the solid state and in selective solvents to afford ordered microstructures that display unique, technologically significant properties in comparison to blends of the respective homopolymers.<sup>[1]</sup> However, the synthetic repertoire of these materials has been limited to tapered blocks of uniform sequence, which potentially restricts the functional complexity of the resulting microstructures. Genetic engineering of synthetic polypeptides enables preparation of block copolymers composed of complex sequences in which the individual blocks may have different mechanical, chemical, or biological properties.<sup>[2–6]</sup> The segregation of the protein blocks into compositionally, structurally, and spatially distinct domains should occur in analogy with synthetic block copolymers, affording ordered structures on the nanometer to micrometer size range. The utility of these protein materials depends on the ability to functionally emulate or enhance the materials properties of conventional polymer systems, while retaining the benefits of greater control over the sequence and microstructure that protein engineering affords for the construction of materials. We

report herein the genetically directed synthesis and characterization of a triblock copolymer **1** that is derived from an elastin-mimetic polypeptide sequence in which the respective blocks exhibit different mechanical properties (Scheme 1). Moreover, the sequences of the respective blocks were chosen



Scheme 1. Amino acid sequence of protein-based block copolymers **1** and **2** derived from elastin-mimetic peptide sequences [24].

such that the polypeptide undergoes reversible microscopic phase separation from aqueous solution to form a thermoplastic elastomer hydrogel above a lower critical solution temperature  $T_c$ .

## 2. Results and Discussion

Elastin-mimetic protein polymers comprise a versatile class of polypeptide materials in which the phase behavior and mechanical properties depend critically on the identity of the residues within the pentapeptide repeat sequence [(Val/Ile)–Pro–Xaa–Yaa–Gly].<sup>[7]</sup> Alterations in the identity of the fourth residue (Yaa) attenuate the position of the lower critical solution temperature of the polypeptide in aqueous solution in a manner commensurate with the effect of the polarity of the amino acid side chain on the polymer–solvent interaction. In addition, substitution of an Ala residue for the consensus Gly residue in the third (Xaa) position of the repeat results in a change in the mechanical response of the material from elastomeric to plastic. The macroscopic effects of these sequence alterations were employed to design an elastin-mimetic polypeptide sequence **1** that mimics triblock copolymers (BAB) that undergo microscopic phase separation to afford thermoplastic elastomer gels.<sup>[8–11]</sup> Polypeptide **1** incorporates identical endblocks of a hydrophobic plastic sequence separated by a central hydrophilic elastomeric block such that the difference in mechanical

[\*] Prof. V. P. Conticello, E. R. Wright, Dr. R. A. McMillan  
Department of Chemistry, Emory University  
Atlanta, GA 30322 (USA)  
E-mail: vcontic@emory.edu

Prof. A. Cooper  
Chemistry Department, University of Glasgow  
Glasgow G12 8QQ, Scotland (UK)

Dr. R. P. Apkarian  
Integrated Microscopy & Microanalytical Facility, Emory University  
Atlanta, GA 30322 (USA)

[\*\*] This research was supported through a grant from the NASA Office of Life and Microgravity Sciences and Applications (NAG8-1579). E.R.W. acknowledges a Department of Education Graduate Assistance in Areas of National Need (G.A.A.N.N.) fellowship. The UK Biotechnology and Biological Sciences (BBSRC) and Engineering and Physical Sciences (EPSRC) Research Councils jointly fund the Biological Microcalorimetry Facility at Glasgow University. We thank Dr. Sarla Goel of Paar Physica for assistance with the dynamic rheology measurements.

properties of the blocks coincides with a difference in polarity, resulting in net amphiphilic character in the polypeptide. The repeat sequence of the endblocks (B) was chosen such that their lower critical solution temperature would reside at or near ambient temperature, which would result in phase separation of the plastic domains from aqueous solution under physiologically relevant conditions.<sup>[7]</sup> The elastomeric repeat unit contains periodically placed glutamic acid residues, which enhance segregation between the two phases in aqueous solution and increase the affinity of the elastomeric domain for the aqueous solvent.<sup>[2]</sup> Protein polymer **1** should reversibly self-assemble from concentrated aqueous solution above the phase transition of the hydrophobic endblocks to form a network of plastic microdomains dispersed in a continuous phase of the elastomeric midblock and solvent. Thus, by combination of the mechanical and solution thermodynamic properties of elastin-derived protein sequences, thermoplastic elastomer hydrogels may be prepared that have an inverse temperature profile for self-assembly in comparison to conventional thermoplastic elastomers.

The assembly of the genetic construct encoding **1** employed a convergent strategy in which identically sized concatemers of the plastic sequence were initially joined together in a modified version of plasmid pET-24a to afford a sequence encoding the diblock polypeptide **2**.<sup>[12]</sup> The short elastin segment between the regions encoding the two endblocks contains a unique cleavage site for the restriction endonuclease *SexA* I. Restriction digestion of the recombinant plasmid with this enzyme generated cohesive ends that were compatible with the deoxyribonucleic acid (DNA) cassettes encoding the elastin-mimetic concatemers that comprised the central block. Enzymatic ligation of a pool of DNA cassettes encoding concatemers of the elastic repeat enriched in high molar mass sequences (2000–4000 base pairs) resulted in isolation of a clone encoding polypeptide **1**. This flexible strategy permits the insertion of DNA cassettes encoding a range of elastin-mimetic sequences [Val–Pro–Gly–Yaa–Gly] into the central site within the triblock copolymer as long as the termini are compatible with those of the *SexA* I-digested plasmid. Expression of the synthetic genes encoding **1** and **2** was performed from the respective plasmids in *E. coli* strain BL21-Gold(DE3) using the hyperexpression protocol of Daniell et al.<sup>[13]</sup> Proteins **1** and **2** were isolated from the bacterial cell lysate in high yield and purity using a repetitive precipitation procedure. Amino acid compositional analysis and matrix-assisted laser desorption ionization time-of-flight mass spectrometry (MALDI-TOF-MS) confirmed the identity of the recombinant polypeptides.<sup>[14]</sup> The <sup>1</sup>H and <sup>13</sup>C nuclear magnetic resonance (NMR) spectroscopic data at 4 °C in aqueous solution were consistent with the proposed sequences of **1** and **2**.

Differential scanning calorimetry (DSC) on dilute aqueous solutions (ca. 1 mg/mL) of **1** and **2** displayed sharp endothermic transitions at 23 °C and 21 °C, respectively, that were virtually independent of the pH of the solution (Fig. 1).<sup>[15]</sup> The transitions are reversible upon cooling and rescan in the calorimeter, though with some indication of sample degradation upon repeated scans to high temperature (data not shown).

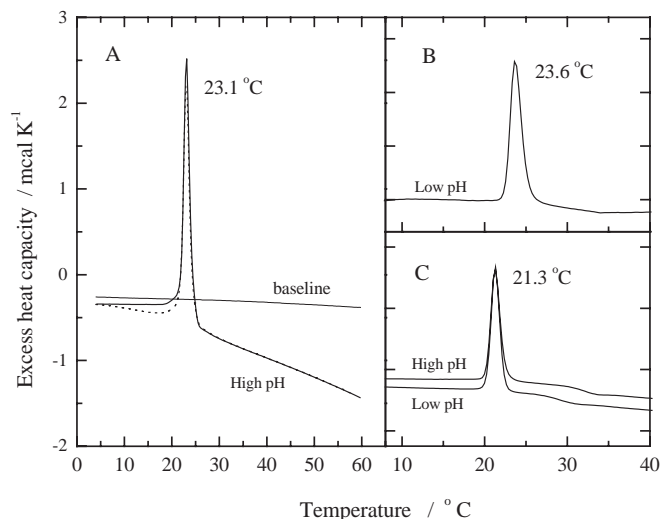


Fig. 1. Raw DSC data for the endothermic thermal transitions of **1** and **2** in dilute aqueous solution. A) Protein **1** at high pH (40 mM NaOH), with rescan (dotted line) showing reversibility. The instrumental baseline is shown for comparison. B) Protein **1** at low pH (40 mM acetic acid). C) Protein **2** at high and low pH. The temperature maximum for each transition is as indicated.

These results are consistent with cooperative van 't Hoff transition enthalpies ( $\Delta H$ ) in the range 400–440 kcal mol<sup>-1</sup> (**1**) or 500–540 kcal mol<sup>-1</sup> (**2**), which indicate an entropy driven (positive  $\Delta S$ ) process that is in line with hydrophobic or other solvation related interactions. The decrease in apparent heat capacity of the polypeptide above the transition temperature (as indicated by the baseline drift in Fig. 1) is characteristic of the cooperative formation of condensed protein aggregates.<sup>[16]</sup> The close correspondence observed between the phase transitions of **1** and **2** suggests that this process involves selective desolvation and ensuing micro-phase separation of the endblock segments. The lack of significant pH dependence for the thermal transition temperature of polypeptide **1** suggests that the glutamate-rich central block of this copolymer is not involved in the transition.

Variable temperature (VT) <sup>1</sup>H–<sup>13</sup>C heteronuclear correlation through multiple quantum coherence (HMQC) NMR spectroscopy confirms that polypeptide **1** undergoes a selective phase transition above a lower critical solution temperature.<sup>[17]</sup> A thorough comparison of the HMQC spectra of **1** at 4 °C and 25 °C indicated that the resonances associated with the hydrophobic endblocks, which are well-resolved at 4 °C, disappear at 25 °C due to micro-phase separation above the inverse temperature transition (see below). This phenomenon can be clearly observed in an expansion of the  $\alpha(\text{CH})$  region of the HMQC NMR spectrum (Fig. 2). The resonances that are associated with the endblock sequences appear only in the low temperature spectrum, while those associated with the central block remain visible both above and below the lower critical solution temperature transition. These results suggest that the endblocks are motionally restricted above the endothermic transition, which is consistent with selective micro-phase separation of these domains from the aqueous solvent. In contrast, the central block remains conformationally flexible and hydrated above the phase transition. Similar effects have been observed

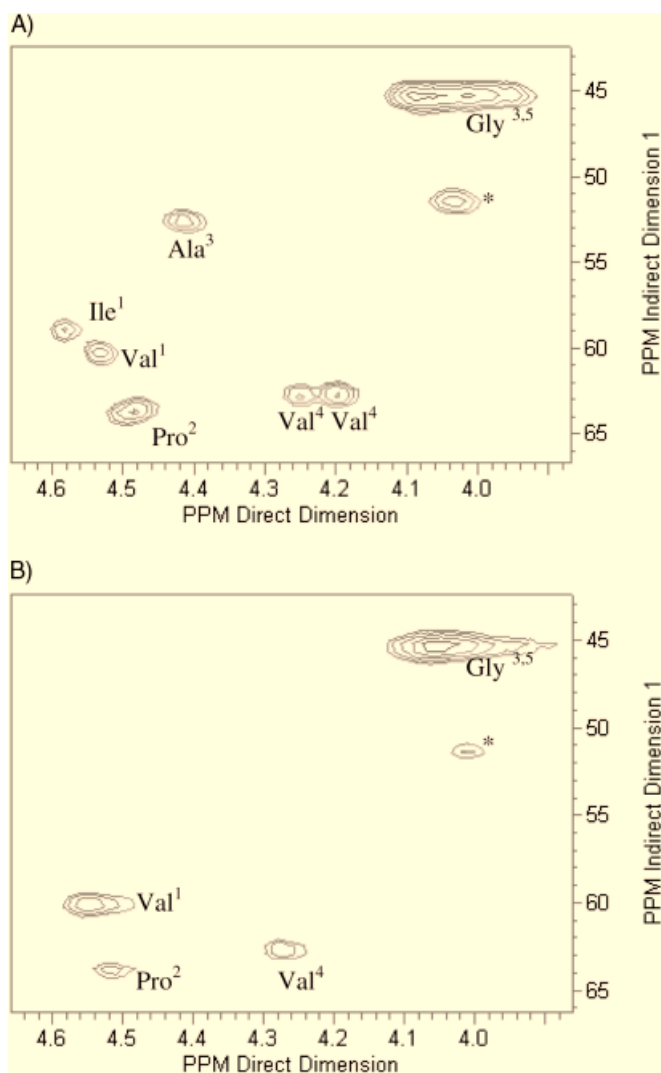


Fig. 2. Comparison of  $(CH)_\alpha$  region of the  $^1H,^{13}C$  HMQC NMR spectra of **1** at 4°C (A) and 25°C (B), which represent temperatures respectively below and above the phase transition of **1**. The asterisk indicates the position of one of the cross-peaks that originate from Pro<sup>2</sup>(CH) $\delta$ .

for an amphiphilic diblock copolymer based on an elastin-mimetic polypeptide sequence, in which selective phase segregation of the more hydrophobic block occurred in conjunction with an endothermic phase transition.<sup>[2a]</sup> Transmission electron microscopy (TEM) measurements of specimens of **1** deposited from aqueous solution at 25°C and selectively stained with 10 mM Cs<sub>2</sub>CO<sub>3</sub> solution indicated a spherical micellar morphology that was consistent with selective aggregation of the endblock domains.

Experimental<sup>[9-11,18]</sup> and computational<sup>[19]</sup> studies of BAB triblock copolymer systems have indicated that, as the concentration of the polymer increases within a midblock-selective solvent, the proportion of endblocks localized within spatially distinct micellar domains increases such that formation of an elastomeric network occurs above a critical concentration. Indeed, the reversible formation of macroscopic gels was observed upon cycling the temperature of concentrated aqueous solutions (20–25 wt.-%) of proteins **1** and **2** through the calori-

metric phase transition. Since this phase transition involves selective segregation of the endblock domains, we hypothesize that under these conditions the fraction of bridging midblocks exceeds the minimal value required for the formation of an elastomeric network. The dynamic rheological properties of these two specimens were studied as a function of temperature in the regime flanking the phase transition (Fig. 3),<sup>[20]</sup> which

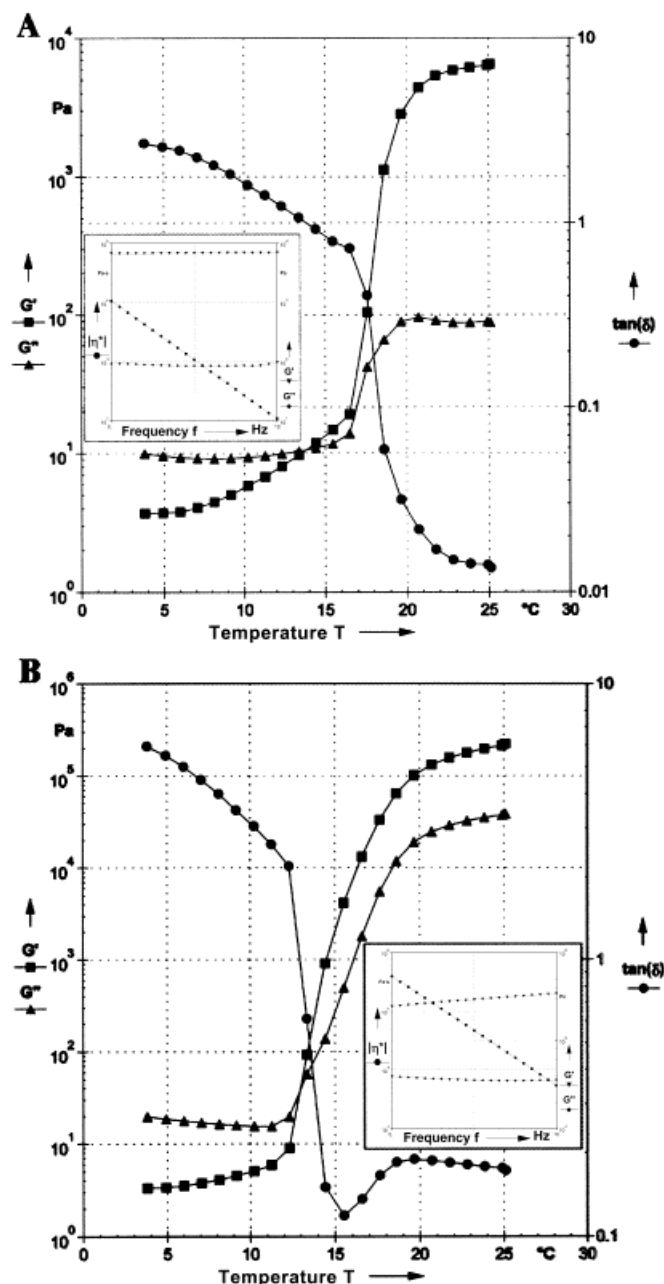


Fig. 3. Dynamic rheological data describing the variation of the storage ( $G'$ ) and loss ( $G''$ ) moduli as a function of temperature for concentrated aqueous (25 wt.-%) solutions of proteins **1** (A) and **2** (B). The insets within the respective figures depict the frequency sweeps for these solutions at 25°C within the indicated range at a strain amplitude of 1%.

revealed interesting correlations as well as significant differences between these structurally related protein materials. Both specimens exhibited an inflection point within the dy-

dynamic mechanical properties as the temperature was raised from 4 °C to 25 °C, which resulted in a crossover of the relative magnitudes of the dynamic storage ( $G'$ ) and loss moduli ( $G''$ ). This crossover was consistent with a transition from a viscoelastic liquid at low temperature (4 °C) to a viscoelastic solid at high temperature (25 °C). Moreover, the position of the inflection point occurred slightly below the respective calorimetric transitions that were observed for the two polymers, which may arise from the greater concentration of these specimens in comparison to those employed in the DSC measurements.

The rheological behavior of protein **1** indicated that it behaved as a gel at 25 °C in that the value of  $G'$  exceeded that of  $G''$  by nearly two orders of magnitude under these conditions. In addition, the corresponding frequency sweeps for solutions of **1** demonstrated a constant value for  $G'$  over two orders of magnitude within the linear viscoelastic regime. In contrast, the rheological behavior of solutions of **2** differed subtly from those of **1**. The difference between  $G'$  and  $G''$  was less than that observed for solutions of **1**, although the absolute magnitude of each parameter was higher than observed for the triblock system. More significantly, the frequency sweeps for the solutions of **2** indicated that  $G'$  was not constant under the same conditions employed for **1**, and a small but significant hysteresis was observed for the values of  $G'$  upon replicate measurement that was not observed for solutions of **1**. These incongruities in rheological behavior between solutions of **1** and **2** may arise due to differences between the respective sequences of the polypeptides. In particular, protein **2** is a virtual homopolymer of the plastic sequence in which two identical endblocks are separated by a short segment consisting of two repeats of the elastin pentapeptide sequence (Scheme 1). The usual model invoked for triblock copolymer gels<sup>[9–11]</sup> involves the formation of a dispersed network of endblock aggregates that act as virtual crosslinks within a matrix consisting of bridging midblocks swollen in a compatible solvent. Clearly, the short central block of protein **2** precludes the adoption of this idealized architecture in contrast to protein **1**, in which the size of the central block approaches that of the sum of the endblock domains.

The morphology of specimens of **1** and **2** in the gel state were determined using cryo high-resolution scanning electron microscopy (cryo-HRSEM) (Figs. 4 and 5).<sup>[21,22]</sup> Both systems display micro-phase separated morphologies that are characterized by the presence of spherical micellar aggregates, which were reproducibly larger in size for gels derived from **1** (20–30 nm in diameter) in comparison to those derived from **2** (15–20 nm in diameter). The micellar particles observed in

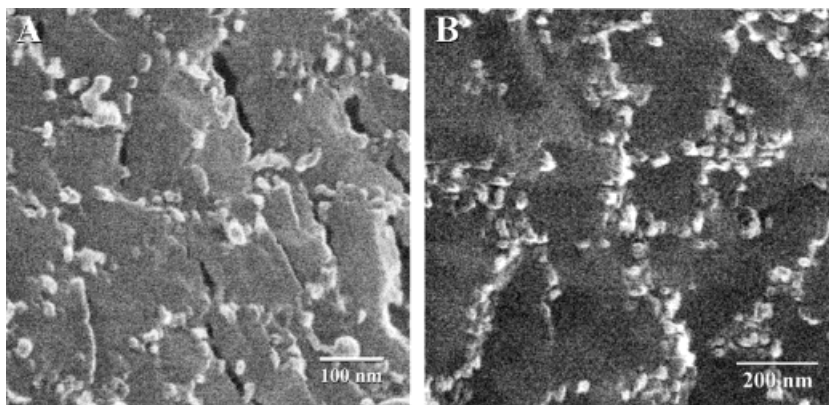


Fig. 4. Cryo-HRSEM images of vitrified specimens of concentrated aqueous (25 wt.-%) solution of proteins **1** (A) and **2** (B) prepared via rapid cryo-immobilization from gel specimens equilibrated at 25 °C.

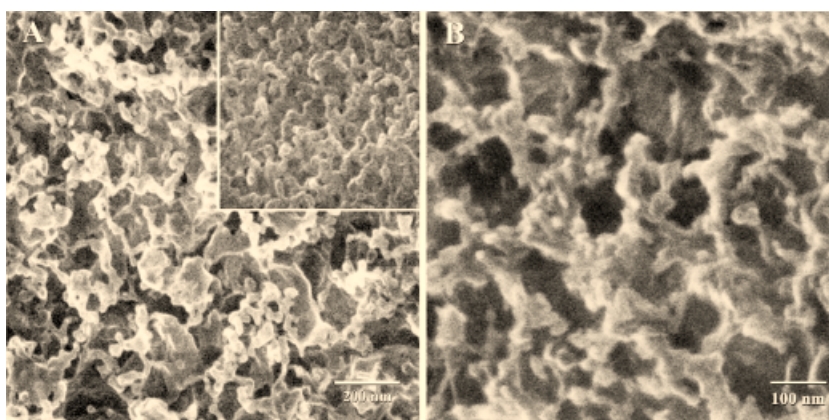


Fig. 5. Cryo-HRSEM images of vitrified specimens of concentrated aqueous (25 wt.-%) solution of proteins **1** (A) and **2** (B) prepared via rapid cryo-immobilization from gel specimens equilibrated at 25 °C. The specimens were etched prior to image acquisition by controlled sublimation of vitreous ice to expose the protein at the interface. The inset in (A) depicts a specimen of protein **1** that had been subjected to a low level of controlled etching, which reveals the underlying symmetry of the protein network.

concentrated solutions of **1** correspond closely in size to those observed by TEM for specimens deposited from dilute solutions of **1** (see above). In contrast, micellar particles were not detected in specimens of **1** that were vitrified from concentrated solutions maintained below the calorimetric phase transition. The latter system displays a uniform morphology that comprises features that are reminiscent of the thin leaflet morphology observed for chemically cross-linked elastin-mimetic proteins that were cryo-immobilized from the low temperature, solvent-swollen state.<sup>[23]</sup> The spectroscopic and calorimetric data clearly indicate that microscopic phase separation of the endblock domains coincides with the endothermic transition, which is consistent with the temperature-dependent morphological properties and rheological behavior of concentrated aqueous solutions of **1**.

The underlying morphology of the protein aggregates within the gels can be more clearly discerned from specimens in which the vitreous ice has been etched from the surface via controlled sublimation (Fig. 5). At low levels of etching (Fig. 5A inset), a uniform and densely packed matrix of interconnected micellar particles can be distinguished within gel specimens of **1**. The metrical features of the particles are similar in aspect to those

observed above for the unetched specimens. Further etching reveals the presence of a network of beaded filaments that consist of interconnected particles that are dispersed fairly evenly at the surface of the specimen. A similar beaded filament morphology has been previously observed for an elastin-mimetic diblock protein above the phase transition of the hydrophobic block,<sup>[2a]</sup> although this material does not behave as a macroscopic gel under conditions that approximate those employed for **1** and **2**. In contrast, the micellar particles in **2** are reproducibly smaller in diameter than those of **1**, as observed in Figure 4, and display a noticeable tendency to form clusters of aggregates (Fig. 5B). The clustering effect may arise due to the short size of the bridging domain between the two endblocks within **2**, which promotes aggregation of the endblock domains. The differences in morphological features between **1** and **2** are thus consistent with the variation in size of the central domain and are manifested at the macroscopic level in the distinctions in dynamical mechanical behavior observed between the two gel systems.

### 3. Conclusion

These experimental data indicate that protein-based analogues of conventional thermoplastic elastomers can be designed with enhanced properties as a consequence of the precise control of primary structure. Protein **1** undergoes a reversible sol–gel transition over a narrow temperature range with an inverse temperature profile, which results in the formation of a well-defined elastomeric network above a lower critical solution temperature. The morphology of the network is consistent with selective microscopic phase separation of the endblock domains, which results in the formation of virtual cross-links that are inter-connected via bridging midblock segments. This genetic engineering approach provides a method for specification of the critical architectural parameters, i.e., block length and sequence, which define macromolecular properties such as the position of the phase transition and the mechanical behavior of the individual blocks that are important for downstream applications. We envision that materials derived from these proteins may be employed for in-vivo applications within biomedical devices, with a greater potential to emulate the functional complexity of native protein materials than the synthetic polymer systems that are currently in use.

### 4. Experimental

Oligonucleotide cassettes encoding the elastic (**A**) and plastic (**B**) (see Table 1) repeat units were independently synthesized and inserted into the *Bam*H I/*Hin*D III sites within the polylinkers of pZErO-1 and pZErO-2, respectively. Recombinant clones were isolated after propagation in *E. coli* strain Top10F', and the sequences of the inserts were verified by double-stranded automated DNA sequence analysis. These clones were propagated in *E. coli* strain SCS110 in order to isolate preparative amounts of plasmid DNA. DNA monomers **A** and **B** were liberated from the respective plasmids via restriction digestion with *Sex*A I and *Bsp*M I, respectively. Self-ligation of each DNA cassette afforded a population of concatemers encoding repeats of the elastic and plastic sequences, respectively. Concatemers derived from DNA monomer B was inserted into the *Bsp*M I site of the modified polylinker **C** in plasmid pET-24a. A concatemer

Table 1. Coding sequences of the oligonucleotide cassettes employed in the construction of proteins **1** and **2**

<b>A</b>	<b>Val</b>	<b>Pro</b>	<b>Gly</b>	<b>Val</b>	<b>Gly</b>	<b>Val</b>	<b>Pro</b>	<b>Gly</b>	<b>Val</b>	<b>Gly</b>	<b>Val</b>	<b>Pro</b>	<b>Gly</b>
	GTA	CCT	GGT	GTT	GGC	GTT	CCG	GGT	GTA	GGT	GTA	CCA	GGC
	CAT	GGA	CCA	CAA	CCG	CAA	GGC	CCA	CAT	CCA	CAT	GGT	CCG
	<b>Glu</b>	<b>Gly</b>	<b>Val</b>	<b>Pro</b>	<b>Gly</b>	<b>Val</b>	<b>Gly</b>	<b>Val</b>	<b>Pro</b>	<b>Gly</b>	<b>Val</b>	<b>Gly</b>	
	GAA	GGT	GTA	CCG	GGT	GTT	GGC	GTA	CCA	GGC	GTT	GGC	
<b>B</b>	<b>Val</b>	<b>Pro</b>	<b>Ala</b>	<b>Val</b>	<b>Gly</b>	<b>Ile</b>	<b>Pro</b>	<b>Ala</b>	<b>Val</b>	<b>Gly</b>	<b>Ile</b>	<b>Pro</b>	<b>Ala</b>
	GTA	CCT	GCT	GTT	GGT	ATT	CCG	GCT	GTT	GGT	ATC	CCA	GCT
	CAT	GGA	CGA	CAA	CCA	TAA	GGC	CGA	CAA	CCA	TAG	GGA	CGA
	<b>Val</b>	<b>Gly</b>	<b>Ile</b>	<b>Pro</b>	<b>Ala</b>	<b>Val</b>	<b>Gly</b>	<b>Ile</b>	<b>Pro</b>	<b>Ala</b>	<b>Val</b>	<b>Gly</b>	
	GTT	GGT	ATC	CCA	GCT	GTT	GGC	ATT	CCG	GCT	GTA	GGT	
<b>C</b>	<b>Met</b>	<b>Val</b>	<b>Pro</b>	<b>Gly</b>	<b>Val</b>	<b>Gly</b>	<b>Val</b>	<b>Pro</b>	<b>Gly</b>	<b>Val</b>	<b>Gly</b>	<b>Val</b>	
	ATG	GTT	CCG	GGT	GTA	GGT	GTA	CCT	GGT	GTT	GGG	GTA	
	TAC	CAA	GGC	CCA	CAT	CCA	CAT	GGA	CCA	CAA	CCC	CAT	
	<b>Pro</b>	<b>Gly</b>	<b>Val</b>	<b>Gly</b>	<b>Ile</b>	<b>Pro</b>	<b>Ala</b>	<b>Val</b>	<b>Gly</b>	<b>Stop</b>	<b>Stop</b>		
	CCT	GCT	GTT	GGT	ATT	CCT	GCA	GTT	GGC	TGA	TGA		
<b>D</b>	<b>Met</b>	<b>Val</b>	<b>Pro</b>	<b>Ala</b>	<b>Val</b>	<b>Gly</b>	<b>Ile</b>	<b>Pro</b>	<b>Ala</b>	<b>Val</b>	<b>Gly</b>	<b>Val</b>	
	ATG	GTA	CCT	GCT	GTT	GGT	ATT	CCT	GCA	GTT	GGC	GTT	
	TAC	CAT	GGA	CGA	CAA	CCA	TAA	GGA	CGT	CAA	CCG	CAA	
	<b>Pro</b>	<b>Gly</b>	<b>Val</b>	<b>Gly</b>	<b>Val</b>	<b>Pro</b>	<b>Gly</b>	<b>Val</b>	<b>Gly</b>	<b>Stop</b>	<b>Stop</b>		
	CCG	GGT	GTA	GGT	GTA	CCT	GGT	GTT	GGG	TGA	TGA		

encoding sixteen repeats of the plastic sequence was isolated and identified via restriction cleavage with *Kpn* I and *Pst* I. Double-stranded DNA sequence analysis confirmed the integrity of the concatemer within the recombinant plasmid, which was labeled pPC. The concatemer was liberated from pPC via restriction cleavage with *Kpn* I and *Pst* I and purified via preparative agarose gel electrophoresis. Enzymatic ligation was used to join the concatemer cassette to the *Kpn* I/*Pst* I sites within the modified polylinker **D** in pET-24a. Double-stranded DNA sequence analysis confirmed the integrity of the concatemer within the recombinant plasmid, which was labeled pPN. The pair of recombinant plasmids pPN and pPC encoded the N-terminal and C-terminal domains of the diblock polymer **2**, respectively. Restriction cleavage of each plasmid with *Sex*A I and *Xma* I afforded two fragments, which were separated via preparative agarose gel electrophoresis. Enzymatic ligation of the large fragment of pPN and the small fragment of pPC afforded the recombinant plasmid pP2, which encoded protein **2** as a single contiguous reading frame within plasmid pET-24a. Plasmid pP2 was propagated in *E. coli* strain SCS110 and cleaved with restriction endonuclease *Sex*A I. Concatemers encoding the elastin sequence **A** were inserted into the compatible *Sex*A I site of pP2. The recombinant clones were analyzed by restriction digestion with *Kpn* I and *Pst* I, followed by agarose gel electrophoresis. A clone was isolated that encoded approximately thirty repeats of the elastic sequence. Plasmid pPEP encoded the triblock copolymer protein **1** as a single contiguous reading frame within plasmid pET-24a. Plasmids pP2 and pPEP were used to transform the *E. coli* expression strain BL21-Gold(DE3). Large-scale fermentation was performed at 37 °C in Terrific Broth (TB) medium supplemented with kanamycin (50 µg/mL) [13]. The target proteins were purified from the whole cell lysate by three to five cycles of temperature-induced precipitation (4 °C/37 °C) from 500 mM NaCl solution. Dialysis and lyophilization afforded proteins **1** and **2** as fibrous solids in isolated yields of 614 mg/L of culture and 781 mg/L of culture, respectively. Sodium dodecyl sulfate–polyacrylamide gel electrophoresis (SDS-PAGE) analysis indicated apparent molar masses of approximately 150 000 Da and 80 000 Da for **1** and **2**, respectively.

**NMR Experiments:** All solution NMR experiments were carried out with samples consisting of 43 mg of protein and 1 mg of sodium 2,2-dimethyl-2-silapentane-5-sulfonate (DSS) as internal standard (0.0 ppm) dissolved in 50:50 sterile H<sub>2</sub>O/D<sub>2</sub>O. Copolymer **1** was maintained at neutral pH whereas copolymer **2** was adjusted to pH 2.7, this adjustment slows the proton exchange rate such that amide protons were observable in the <sup>1</sup>H NMR spectra. Samples were recorded at 4 °C and 25 °C. Standard solvent suppression techniques were employed to

reduce signal due to the residual protons of water in the  $^1\text{H}$  NMR of aqueous solutions. The HMQC NMR experiments were acquired at 4 °C and 25 °C with a 90° pulse of 8  $\mu\text{s}$  on the proton (sweep width 5500.2 Hz) and a 90° pulse of 12  $\mu\text{s}$  on the carbon. The data matrix contained 256  $t_1$  increments (sweep width in  $F_1$  (carbon), 33 999.2 Hz) at 96 scans per increment. The NMR data were processed using the program NutsPro from Acorn NMR, Inc. (Livermore, CA).

**Rheology Measurements:** A parallel plate arrangement was employed in which the plate had a diameter of 24.94 mm, a concentricity of 6  $\mu\text{m}$ , and a parallelity of 3  $\mu\text{m}$ . Samples of the polypeptides were prepared as 20–25 wt.-% solutions of protein in sterile, deionized  $\text{H}_2\text{O}$  and were equilibrated at 4 °C prior to the measurements. Approximately 300  $\mu\text{L}$  of the sample was applied to the bottom plate of the rheometer. The top plate was lowered to a distance of 0.5 mm. Silicon oil was applied around the plate and sample's circumference in order to prevent evaporative loss of solvent from the sample during the measurements. Three different tests were performed sequentially as follows. Temperature sweeps were recorded from 3 °C to 25 °C over a period of eleven minutes in duration (0.5 min at each temperature) with a strain of 1% at an angular frequency of 10 rad/s. Replicate measurements were recorded under identical conditions to ensure reproducibility of the temperature response. Amplitude sweeps of thirty measurements were taken with strains ( $\gamma$ ) ranging from 0.1 to 100% at an angular frequency ( $\omega$ ) of 10 rad/s. Frequency sweeps of twenty-one measurements at 1% strain were recorded at 25 °C with the frequency ranging from 0.1 to 10 Hz was taken. The frequency sweep was repeated seven times before the plate and sample was cooled to 3 °C in order to duplicate all the experiments.

**Cryo HRSEM Experiments:** Approximately 5 to 10  $\mu\text{L}$  of the solutions were pipetted into 3 mm gold planchets (Balzers BU 012 130T) that had been pre-equilibrated to 4 °C in an isothermal environmental cooler. The temperature of the cooler was raised to approximately 25 °C and allowed to stabilize for 10 min. The solidified samples were plunged into liquid ethane at its melting point (−183 °C) and the vitrified samples were stored in liquid nitrogen ( $\text{LN}_2$ ). A sample was transferred to and mounted on the precooled (ca. −170 °C) Oxford CT-3500 cryo-stage held in the cryo-preparation chamber. The specimen was fractured with a prechilled blade and washed with  $\text{LN}_2$ . The shutters on the stage were closed to minimize frost contamination and the cryo-stage was transferred to the Denton DV-602 Cr coater. At this point, if the samples were to be etched in order to remove excess water (vitreous ice), the stage was allowed to equilibrate in a vacuum of  $\sim 10^{-7}$  torr. Once this occurred, the shutters were opened and the stage was brought to a temperature between −105 °C and −99 °C for varying time intervals. The stage shutters were closed and the stage was returned to −170 °C. A monatomic (1 nm) film of chromium was sputter coated onto the specimen, the stage shutters were closed and the stage was transferred to the upper stage of the DS-130F field-emission SEM operated at 25 kV. During the imaging process, specimen temperature was maintained at −115 °C. Images were digitally collected (5 Mbytes) in 16 s in order to reduce radiation damage.

Received: December 17, 2001

- [1] F. S. Bates, G. H. Fredrickson, *Annu. Rev. Phys. Chem.* **1990**, *41*, 525.
- [2] a) T. A. T. Lee, A. Cooper, R. P. Apkarian, V. P. Conticello, *Adv. Mater.* **2000**, *12*, 1105. b) Y. Qu, S. C. Payne, R. P. Apkarian, V. P. Conticello, *J. Am. Chem. Soc.* **2000**, *122*, 5014.
- [3] a) A. Panitch, T. Yamaoka, M. J. Fournier, T. L. Mason, D. A. Tirrell, *Macromolecules* **1999**, *32*, 1701. b) W. A. Petka, J. L. Harden, K. P. McGrath, D. Wirtz, D. A. Tirrell, *Science* **1998**, *281*, 389.
- [4] a) J. Cappello, J. W. Crissman, M. Crissman, F. A. Ferrari, G. Textor, O. Wallis, J. R. Whitlege, X. Zhou, D. Burman, L. Aukerman, E. R. Steudronsky, *J. Controlled Release* **1998**, *53*, 105. b) J. Cappello, *MRS Bull.* **1992**, *17*, 48. c) J. Cappello, J. Crissman, M. Dorman, M. Mikolajczak, G. Textor, M. Marquet, F. Ferrari, *Biotechnol. Prog.* **1990**, *6*, 198.
- [5] a) S. Winkler, D. Wilson, D. L. Kaplan, *Biochemistry* **2000**, *39*, 12739. b) S. Winkler, S. Szela, P. Avtges, R. Valluzzi, D. A. Kirschner, D. Kaplan, *Int. J. Biol. Macromol.* **1999**, *24*, 265.
- [6] a) D. E. Meyer, K. Trabbic-Carlson, A. Chilkoti, *Biotechnol. Prog.* **2001**, *17*, 720. b) D. E. Meyer, A. Chilkoti, *Nat. Biotechnol.* **1999**, *17*, 1112.
- [7] D. W. Urry, C.-H. Luan, C. M. Harris, T. M. Parker, in *Protein-Based Materials* (Eds: K. McGrath, D. Kaplan), Birkhauser, Boston, MA **1997**, Ch. 5.
- [8] R. J. Spontak, N. P. Patel, *Curr. Opin. Colloid Interface Sci.* **2000**, *5*, 334.
- [9] a) N. Mischenko, K. Reynders, K. Mortensen, R. Scherrenberg, F. Fontaine, R. Graulus, H. Reynaers, *Macromolecules* **1994**, *27*, 2345. b) N. Mischenko, K. Reynders, M. H. J. Kock, K. Mortensen, J. S. Pedersen, F. Fontaine, R. Graulus, H. Reynaers, *Macromolecules* **1995**, *28*, 2054. c) K. Reynders, N. Mischenko, K. Mortensen, N. Overbergh, H. Reynaers, *Macromolecules* **1995**, *28*, 8699. d) R. Kleppinger, K. Reynders, N. Mischenko, N. Overbergh, M. H. J. Koch, K. Mortensen, H. Reynaers, *Macromolecules* **1997**, *30*, 7008.
- [10] a) J. H. Laurer, R. Buovnik, R. J. Spontak, *Macromolecules* **1996**, *29*, 5760. b) J. H. Laurer, J. F. Mulling, S. A. Khan, R. J. Spontak, R. Bukovnik, *J. Polym. Sci., Part B: Polym. Phys.* **1998**, *36*, 2379. c) J. H. Laurer, J. F. Mulling, S. A. Khan, R. J. Spontak, J. S. Lin, R. Bukovnik, *J. Polym. Sci., Part B: Polym. Phys.* **1998**, *36*, 2513. d) J. H. Laurer, S. A. Khan, R. J. Spontak, M. M. Satkowski, J. T. Grothaus, S. D. Smith, J. S. Lin, *Langmuir* **1999**, *15*, 7947.
- [11] a) J. R. Quintana, E. Diaz, I. Katime, *Macromol. Chem. Phys.* **1996**, *197*, 3017. b) J. R. Quintana, M. D. Janez, I. Katime, *Polymer* **1998**, *39*, 2111. c) J. R. Quintana, E. Diaz, I. Katime, *Polymer* **1998**, *39*, 3029.
- [12] Synthetic methods used to produce the DNA inserts that encode the various elastin block copolymers have been described previously [2a]. For a short description see Experimental section.
- [13] H. Daniell, C. Guda, D. T. McPherson, X. Zhang, J. Xu, D. W. Urry, *Methods Mol. Biol.* **1997**, *63*, 359.
- [14] Amino acid compositional analysis. **1**; Calc. [mol-%]: Ala, 10.4; Glx, 1.9; Gly, 29.6; Ile, 8.2; Pro, 20.0; Val, 29.9. Obs. [mol-%]: Ala, 11.14; Glx, 2.9; Gly, 29.62; Ile, 9.64; Pro, 17.66; Val, 29.51. **2**; Calc. [mol-%]: Ala, 19.8; Gly, 20.2; Ile, 15.7; Pro, 20.0; Val, 24.3. Obs. [mol-%]: Ala, 19.7; Gly, 20.1; Ile, 14.9; Pro, 21.6; Val, 23.7. MALDI-TOF-MS, Obs. (Calc.): **1**, 134097 (134438); **2**, 72016 (72116).
- [15] Copolymer samples for DSC (ca. 1 mg/mL) were dissolved at 4 °C in either 40 mM NaOH or 40 mM ethanoic (acetic) acid and thermal transition data recorded over a temperature range from 4 °C to 60 °C using a Microcal VP-DSC instrument at a scan rate of 1 °C/min. Reversibility was tested by cooling and re-scan of samples in situ. Data were processed and analyzed using Microcal ORIGIN software.
- [16] A. Cooper, *Biophys. Chem.* **2000**, *85*, 25.
- [17] High-resolution solution NMR spectra were acquired on a Varian INOVA 600 (600 MHz,  $^1\text{H}$ ; 150 MHz  $^{13}\text{C}$ ) instrument. The method is described in the Experimental section.
- [18] Z. Tuzar, C. Konák, P. Stepánek, J. Pleštil, P. Kratochvíl, K. Procházka, *Polymer* **1990**, *39*, 3029.
- [19] a) S. H. Kim, W. H. Jo, *Macromolecules* **2001**, *34*, 7210. b) M. Nguyen-Misra, W. L. Mattice, *Macromolecules* **1995**, *28*, 6976. c) M. Nguyen-Misra, W. L. Mattice, *Macromolecules* **1995**, *28*, 1444.
- [20] Rheology measurements were performed on a Paar Physica MCR 300 instrument. See Experimental section for details.
- [21] Cryo-HRSEM measurements were performed on copolymers **1** and **2**, which were prepared as 20 to 25% protein solutions in deionized  $\text{H}_2\text{O}$  at 4 °C. A short description is given in the Experimental section.
- [22] R. P. Apkarian, K. L. Caran, K. A. Robinson, *Microsc. Microanal.* **1999**, *5*, 197.
- [23] R. A. McMillan, K. L. Caran, R. P. Apkarian, V. P. Conticello, *Macromolecules* **1999**, *32*, 9067.
- [24] Abbreviations for amino acids: A, alanine; E, glutamic acid; G, glycine; I, isoleucine; P, proline; and V, valine.